

Microwave modelling and measurement of prematch circuitry for RF power transistors

K. Mouthaan, R. Tinti, H.C. de Graaff, J.L. Tauritz, J. Slotboom
Laboratory of Electronic Components, Technology and Materials
Delft University of Technology, Feldmannweg 17, 2600 GB Delft, The Netherlands.
Phone: +31-15-2784939, Fax: +31-15-2622163, Email: K.Mouthaan@et.tudelft.nl

1 Abstract

The modelling and measurement of prematch circuitry of RF power transistors is considered. Physical models for the bondwires and the prematch capacitor are used to compute resonance frequencies. The models are implemented in Hewlett Packard's Microwave Design System (MDS) and allow designers to predict and optimise the response of the prematch circuitry without fitting of parameters. Differences in modelled and measured resonance frequencies of less than 30 MHz at 1.4 GHz are reported.

2 Introduction

Microwave power transistors are used in base stations to amplify RF signals to power levels of a few Watts or more. In figure 1 a SEM photo of a bipolar power transistor is shown. On the left the input of the transistor, the base, is shown and on the right the output, the collector, is shown. In this photo the intrinsic transistor (the die), the bondwires and the prematch capacitor are visible. The prematch circuitry is the combination of the capacitor and the bondwires and is used in microwave power transistors to transform the low input impedance of the die to a higher impedance at the input of the packaged transistor. A close-up of the prematch capacitor with the bonding wires is shown in figure 1 on the right. A prematch capacitor consists of a block of doped silicon with two contacts (cf. figure 2 on the left). The first contact consists of a thin layer of silicon dioxide (SiO_2) and a wide metal strip (Au) forming a Metal-Oxide-Semiconductor (MOS) capacitor. The second contact is metal (Au) directly on the silicon forming an ohmic contact. Note that in practise the gold is not directly attached to the silicon, additional metals are used to avoid diffusion of the gold into the silicon. If the conduction of the silicon is small a transverse model as shown in figure 2 on the left may be used. In our case however the resistivity of the silicon is low (1-3 m Ω -cm), introducing skin effect behaviour at higher frequencies as is shown later.

In figure 2 on the right the prematch circuit is shown schematically. Bondwires interconnect the package, the prematch capacitor and the die. Normally prematch circuitry is designed by trial and error since predictive models for the wires and the prematch capacitor are not available in standard simulators. With increasing computing power and the drop in the price of RAM, it should be possible in principle to solve for the multiport scattering parameters with a rigorous simulator. In practical situations however this is somewhat cumbersome. In this contribution the modelling of bondwires and the prematch capacitor is considered. The models are implemented in Hewlett Packard's Microwave Design System (MDS) and allow designers to predict and optimise the response of the prematch circuits.

3 Modelling of bondwires

The N coupled bondwires are modelled by an inductance matrix \mathbf{L} in series with a resistance matrix \mathbf{R} forming a $2N$ -port network (cf. figure 3.a). The computation of the inductance matrix is based on Neumann's inductance formula for closed loops [1], [2]. Open loops can be treated using the concept of partial inductance [3]. The inductance formula considers two closed loops of thin wires with the contour C_i defining the center of the current carrying wire i and the contour C_j defining the interior edge of closed loop j . The mutual inductance between these two loops is then given by:

$$L_{ij} = \frac{\text{flux linking } C_j \text{ due to a current in } C_i}{\text{current in } C_i} = \frac{\mu_0}{4\pi} \oint_{C_i} \oint_{C_j} \frac{dl_i \cdot dl_j}{r} \quad (1)$$

where r is the distance between the points on the contours C_i and C_j . To calculate the self inductance the radius of the wire is the distance between the two contours. In our application a loop is formed by considering the image of the bondwire in the ground plane i.e. the wire is mirrored in the ground plane and the computed inductance for this loop is divided by a factor 2. Using Grover's formulation [4] the inductance of a loop is computed by breaking the wire into a set of straight segments and computing equation (1) on a piece-wise basis. Although several approximations are made it was found that both self inductance and mutual inductance of coupled wires are modelled quite accurately compared to measurements [5]. To simplify computation of the resistance matrix, only the diagonal elements are used to model DC and skin losses. Based on the above equations a model for coupled bondwires has been implemented in MDS. This model allows designers to predict and optimise bondwire behaviour in RF power sections [6].

4 Modelling of prematch capacitors

The prematch capacitors consist of two long metal contacts. The first contact forms the MOS capacitor and the second contact is a metallisation layer directly on the silicon forming a low ohmic contact. Only the capacitor contact is modelled using the transmission line shown in figure 3.b. If the conductivity of the silicon is low, the model for an incremental piece of line is shown in figure 3.c. The prematch inductance and resistance per unit length are indicated by L_{pm} and R_{pm} respectively. The silicon dioxide is modelled by the capacitance C_{SiO_2} , and the silicon by the parallel combination of the capacitance C_{Si} and resistance R_{Si} . For this model three characteristic frequencies are defined [7]: the substrate relaxation frequency f_e , the interfacial relaxation frequency f_s and the substrate skin effect frequency f_δ . Based on a parallel plate approximation these frequencies are calculated as: $f_e = 8 \cdot 10^{13}$ Hz, $f_s = 4 \cdot 10^{11}$ Hz and $f_\delta = 130$ MHz. (Data used: $\sigma_{Si} = 5 \cdot 10^4$ S/m, $t_{SiO_2} = 350$ nm and $t_{Si} = 200$ μ m). Silicon substrate resistive effects dominate over capacitive effects as indicated by the substrate relaxation frequency. It is further concluded from f_s that the silicon dioxide dominates the transversal behaviour. Finally from f_δ it is concluded that above approximately 130 MHz skin effect in the substrate comes into play introducing longitudinal currents below the metal contact.

Sonnet's Em 2D planar simulator was used to extract the per unit length values of the transmission line parameters. The structure of interest is shown on the left in figure 4. Although Sonnet's Em does allow the simulation of brick shaped dielectrics, this was found impracticable in the case at hand and the layered structure shown on the right was simulated. In this structure the current flow at the sidewalls of the silicon is not accounted for. The extracted prematch inductance L_{pm} and resistance R_{pm} versus frequency are shown in figure 5. The trace R_s displays the resistance when only the conductivity of the substrate is included i.e. the metal is assumed perfectly conducting. The trace $R_{DC} + R_s$ shows the resistance if the DC resistance of the metal is also included. The resistance is therefore mainly dominated by the longitudinal skin effect current in the substrate. Although not shown in the figure the extracted silicon dioxide capacitance was found to be around 51.7 nF/m. The initial model (figure 3.c) is modified to the model shown in figure 3.d. In this model the upper line corresponds to current flow in the metal and the lower line corresponds to the longitudinal current in the substrate. This current introduces a reactive component modelled by an internal inductance $L_i = R_s/\omega$. The internal inductance L_i and the inductance $L_{pm} - L_i$ are plotted in figure 5. Because the internal inductance L_i dominates, the effect of the normal substrate inductance L_s and the mutual coupling M_L is neglected and the model is reduced to the final transmission line model of figure 3.e.

To use the model in MDS a two coupled lines model is used. The first line models the metal contact and the second line models the current flow in the substrate. The following TEM matrices are used:

$$\mathbf{R} = \begin{bmatrix} R_{DC} & 0 \\ 0 & R_s \end{bmatrix} \quad \mathbf{L} = \begin{bmatrix} L_{pm} - L_i & 0 \\ 0 & L_i \end{bmatrix} \quad \mathbf{C} = \begin{bmatrix} C_{SiO_2} & -C_{SiO_2} \\ -C_{SiO_2} & C_{SiO_2} \end{bmatrix} \quad (2)$$

The diagonal elements of the resistance matrix \mathbf{R} describe loss in the metal and the substrate respectively. The diagonal elements of the inductance matrix \mathbf{L} describe the inductive effect due to current flow in the metal and in the substrate respectively. And the capacitance matrix \mathbf{C} represents the MOS capacitance between the two lines. The conductance matrix is set to zero since current flow between the two lines and current flow from the lines to the ground plane are assumed negligible. The values of the elements of the matrices should be extracted from rigorous simulations or, if possible, from measurements. They can also be computed from simplified expressions.

5 Model verification

Since it is difficult to verify the model by measurement, Hewlett Packard's field simulator package High Frequency Structure Simulator (HFSS) version 5 was used to generate idealised data. This package computes fields rigorously based on finite elements. The first structure under consideration is shown in figure 8. The prematch capacitor is excited by a transmission line on both sides. Although in practise the capacitor is not used in this way, it allows the verification of modelling of transmission line phenomena. The two-port scattering parameters are computed with HFSS, the model and a lumped shunt capacitor of 154.4 pF. Based on these parameters the magnitude of S_{11} and the phase of S_{21} are plotted in figure 6. From these pictures it is observed that the lumped ideal capacitor model is only valid up till a few hundred MHz. Above ≈ 500 MHz other effects come into play. It is also found that the transmission line model predicts the behaviour reasonably well. Above 5 GHz large differences between the model and the HFSS computations occur.

In the second example a single bondwire is connected to the center and the far end of the capacitor respectively. The reflection scattering parameter is calculated with HFSS and compared with the models for the bondwire and the capacitor. For reason of convenience the S_{11} is renormalised to 1 Ω . The computed inductance of the bondwire is 0.8 nH which resonates around 450 MHz with the 154 pF capacitor. The magnitude of S_{11} is plotted in figure 7 (the structures are shown in the insets). For the first configuration resonance frequencies of 430 MHz and 440 MHz are computed with HFSS and the models respectively. The equivalent series resistance at resonance are 0.045 Ω and 0.067 Ω respectively. The resonance frequency for the second configuration is 430

Mhz (HFSS) and 420 MHz (model) and the equivalent series resistance is 0.2Ω and 0.3Ω respectively. Relatively large differences are found in this case between the modelled and computed equivalent series resistance at resonance. By including the side-wall effects the model may be improved. Note also that the model predicts reasonably the factor 4 scaling of the equivalent series resistance, from the first to the second situation.

6 Measurements

As an example the models are compared with microwave measurements of seven samples consisting of a bondwire and a 10 pF prematch capacitor. The samples are mounted in a coplanar setup for accurate characterisation using Cascade Microtech ground-signal-ground probes with $100 \mu\text{m}$ pitch. This setup avoids the contacting problems associated with normal microstrip fixtures and it reduces some distributed effects which can influence the measurements. The coplanar transmission line is characterised by measuring two-port parameters of several transmission lines with differing lengths. The measurements are de-embedded for these coplanar lines. A top view photo and a side view photo are made of each sample to obtain geometrical data and this data is the input for the bondwire model. The prematch capacitor simulations, carried out in Em, use process data from production. Physical data includes the thickness of the SiO_2 layer, relevant dimensions and the conductivity of the silicon block.

S-parameter measurements between 45 Mhz and 10 GHz have been used to determine the S_{11} resonance frequencies. The predicted and measured resonance frequencies are shown in figure 8 for seven different samples. Differences less than 30 MHz at a resonant frequency of circa 1.4 GHz are found. The main explanation for the differences are the limited accuracy of the geometric measurement and the phase error in the S_{11} -parameter.

7 Conclusion and discussion

In conclusion, modelling of prematch circuitry for RF power transistors is considered. The bondwires are modelled with an inductance matrix and a resistance matrix. The elements of the inductance matrix are computed using Neumann's inductance equation. Closed form expressions for the DC and RF resistance are used for the diagonal elements of the resistance matrix. The prematch capacitor is modelled with a transmission line. In case of a highly conducting silicon substrate ($\rho = 1\text{-}3 \text{ m}\Omega\text{-cm}$) the silicon dioxide capacitance mainly dominates the transverse behaviour and the current in the substrate dominates the longitudinal behaviour. This substrate current is modelled by a substrate resistance and an internal inductance. Comparison with rigorous simulations indicates that the model accurately describes the dominant phenomena well.

One of the main problems in the modelling is the assessment of side wall contributions. These walls conduct current to the ground or to the bottom side of the capacitor. An initial attempt to simulate this effect with Sonnet's Em unfortunately failed and 2D simulations with HFSS were also not successful. A second point is the modelling of the ohmic contact. It is anticipated that the substrate current between this contact and the capacitance contact can be modelled with a frequency dependent resistance and an internal inductance. In this case the side wall effects should also be accounted for. Please note that the transmission line only accounts for two dimensional effects. Rigorous simulations may help to find the effect of three dimensional effects, which especially occur if the length of the contact is in the order of the width. The measurements were restricted to rather simple configurations to eliminate undesired effects in the layout of the coplanar structure. Once a good multiport model for the coplanar footprint has been derived, a comparison between the model and measurement of more complex situations is possible.

This work was funded by the Dutch Technology Foundation (STW) under grant nr. DEL 33.3152 and supported by Philips Semiconductors, Nijmegen, the Netherlands.

References

- [1] R.E. Collin, *Field Theory of Guided Waves, second Edition*, 1991, IEEE Press, New York.
- [2] R. Plonsey and R.E. Collin, *Principles and Applications of Electromagnetic Fields*, 1961, McGraw-Hill Book Company, Inc., New York.
- [3] A.E. Ruehli, *Inductance Calculations in a Complex Integrated Circuit Environment*, September 1972, IBM J. Res. Develop, pp. 470-481.
- [4] F. W. Grover, *Inductance Calculations Working Formulas and Tables*, 1946, Dover Publications, Inc., New York.
- [5] K. Mouthaan et al., *Microwave modelling and measurement of the self- and mutual inductance of coupled bondwires*, BCTM 1997, Minneapolis.
- [6] A.O. Harm, E. Aziz, K. Mouthaan and M. Versleijen, *Modelling and simulation of hybrid RF circuits using a versatile compact bondwire model*, October 5-9 1998, European Microwave Conference, Amsterdam.
- [7] H. Hasegawa, M. Furukawa, H. Yanai, *Properties of microstrip line on Si-SiO₂ system*, November 1971, IEEE Trans. on MTT, Vol MTT-19, no. 11, pp. 869-881.

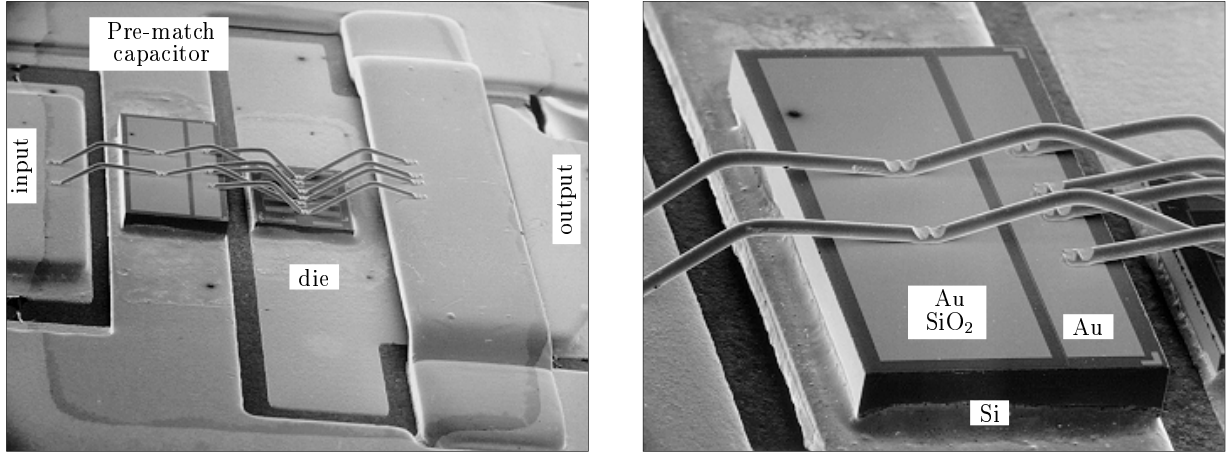


Figure 1: On the left a SEM photo of a RF power transistor with a prematch capacitor and the die. Bondwires are used to interconnect the components. On the right a close up of the prematch capacitor and the bondwires.

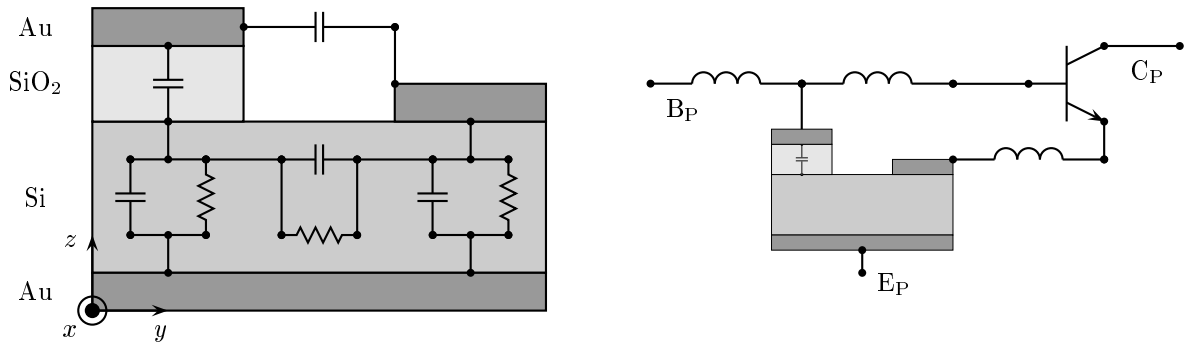


Figure 2: Shown on the left a schematic cross section of the prematch capacitor showing the MOS contact and the ohmic contact. On the right the schematic shows how the connection of bondwires and the capacitor forms the prematch circuit at the input of the transistor.

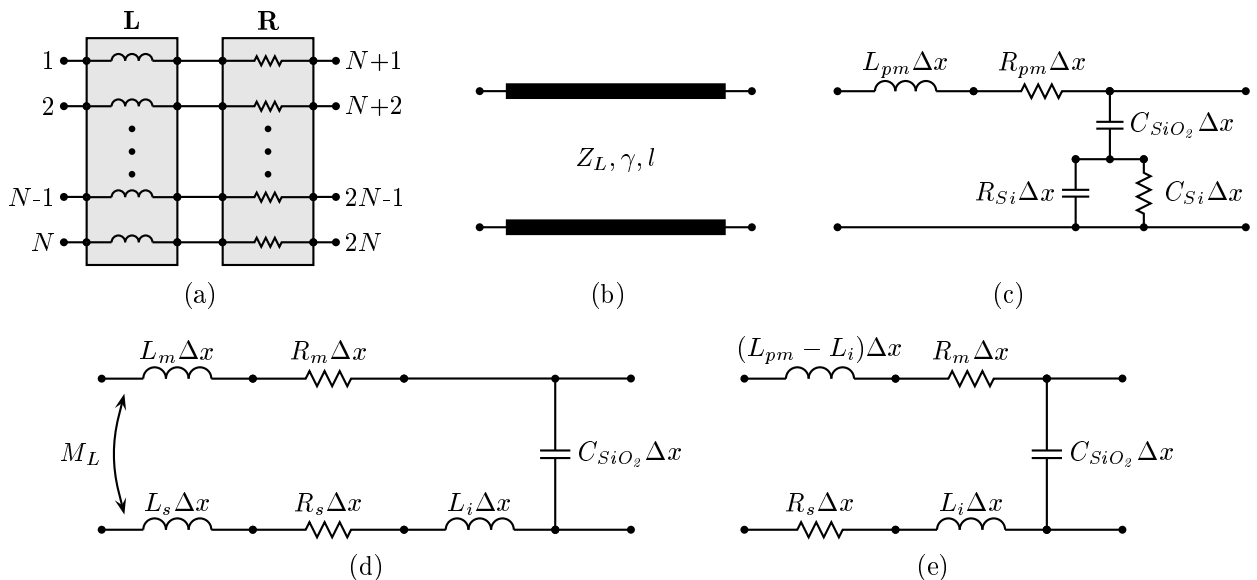


Figure 3: Models for the bondwires and the capacitor. Coupled bondwires are modelled by an inductance matrix \mathbf{L} and a resistance matrix \mathbf{R} (fig. (a)). The capacitor is modelled by a transmission line (fig. (b)), and in case of low substrate conductivity the model of an incremental piece of line is shown in fig. (c). If the substrate is highly conducting the internal inductance L_i is accounted for (d). For reasons of simplicity this model is further reduced as shown in figure (e).

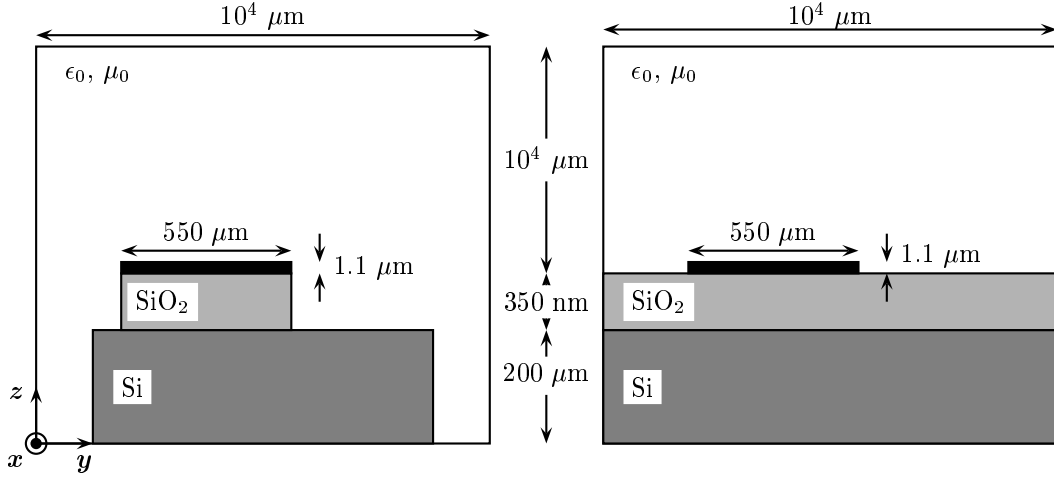


Figure 4: Modelling of the MOS contact in Sonnet's Em. On the left a cross sectional view of the structure of interest. Because the accurate simulation of brick shaped objects in Sonnet's Em in this specific case is complicated, the structure is reduced to a layered medium as shown on the right.

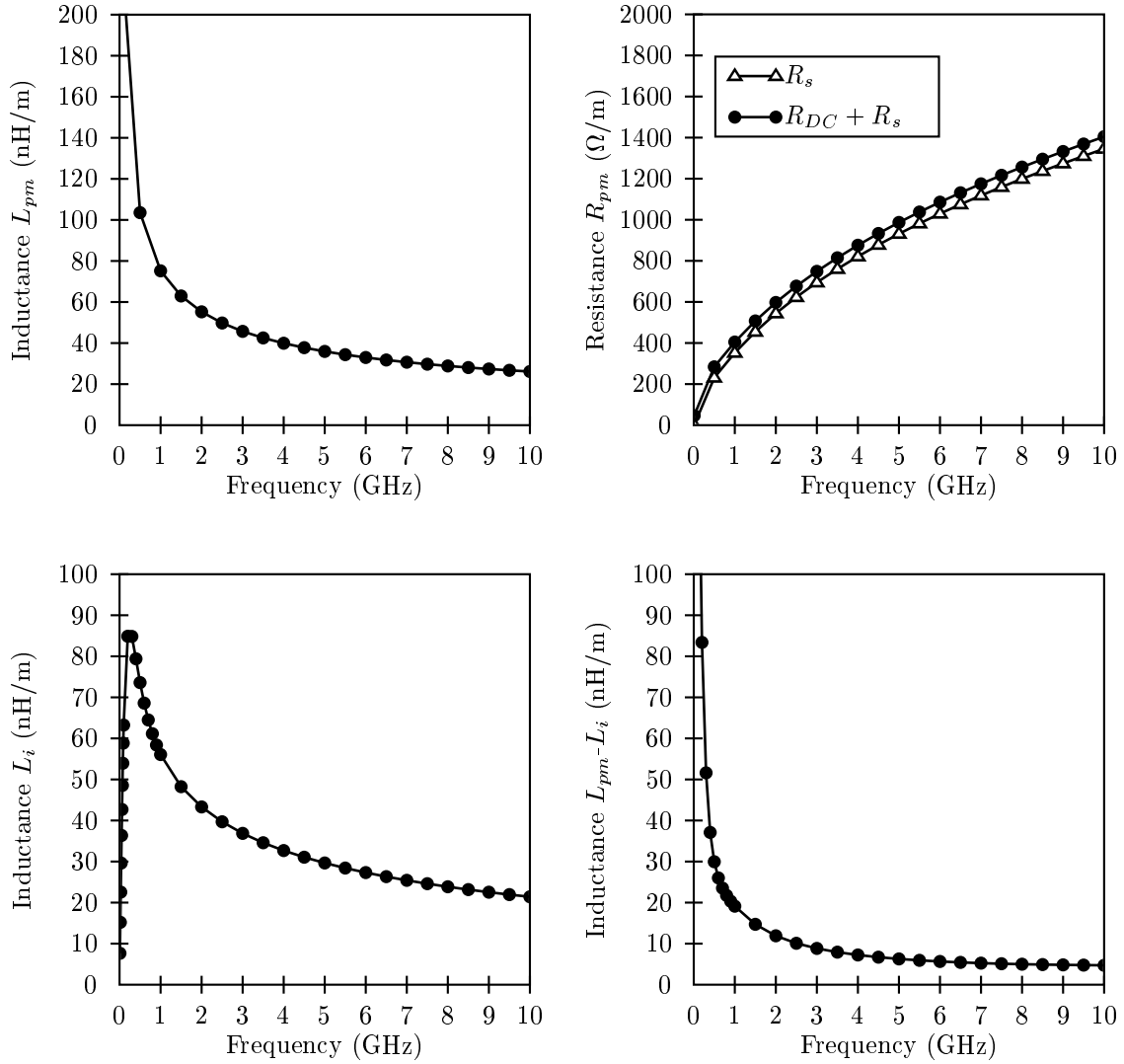


Figure 5: Per unit length quantities versus frequency extracted from the Sonnet Em simulation results. The prematch inductance L_{pm} is shown in the top left graph. The series resistance R_{pm} is shown on the top right. The trace R_s indicates the resistance due to the substrate and the trace $R_s + R_{DC}$ represents the substrate plus the DC resistance of the metal. The internal inductance $L_i = R_s/\omega$ is shown to the bottom left, and the last graph shows the inductance $L_{pm} - L_i$.

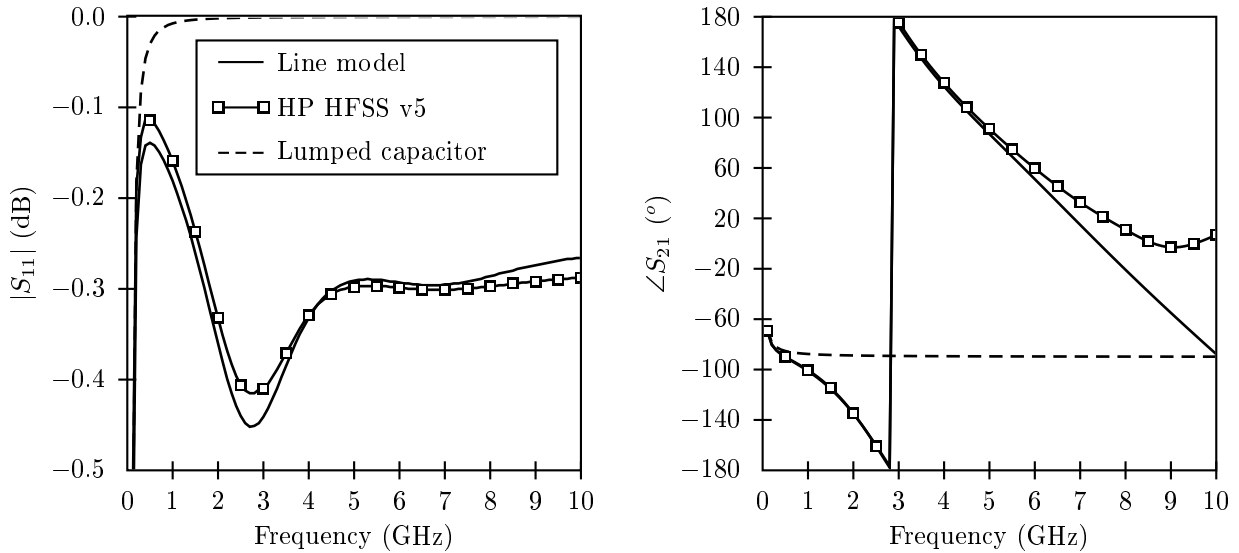


Figure 6: Scattering parameters of a prematch capacitor computed with HP HFSS v5, the transmission line model and a lumped shunt capacitor of 154 pF.

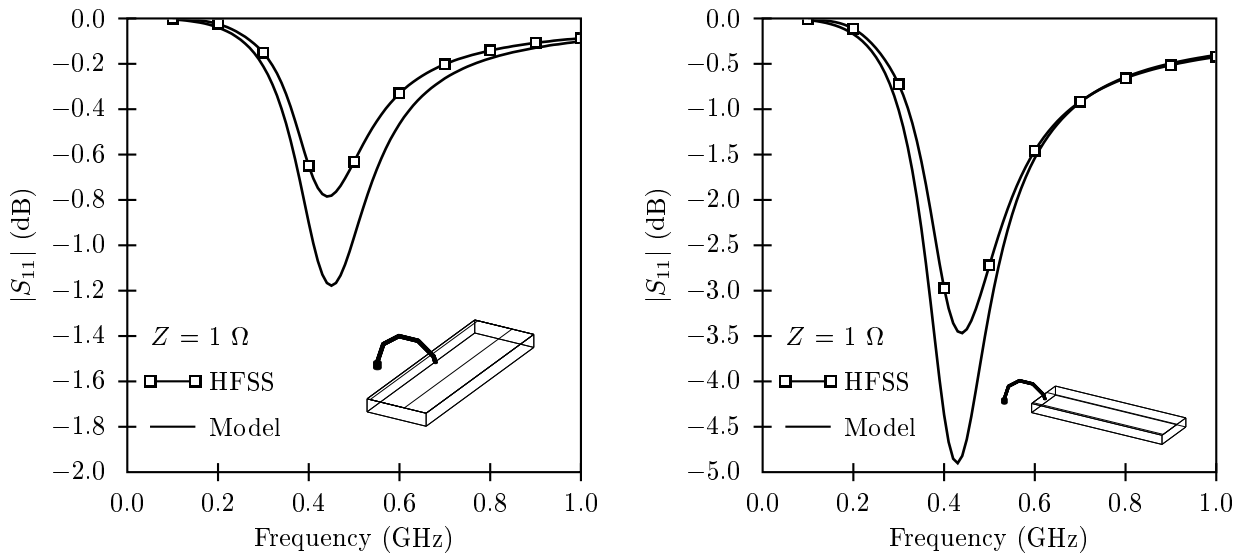


Figure 7: Comparison of modelled and simulated (HFSS) magnitude of S_{11} versus frequency for two different configurations in a 1Ω environment.

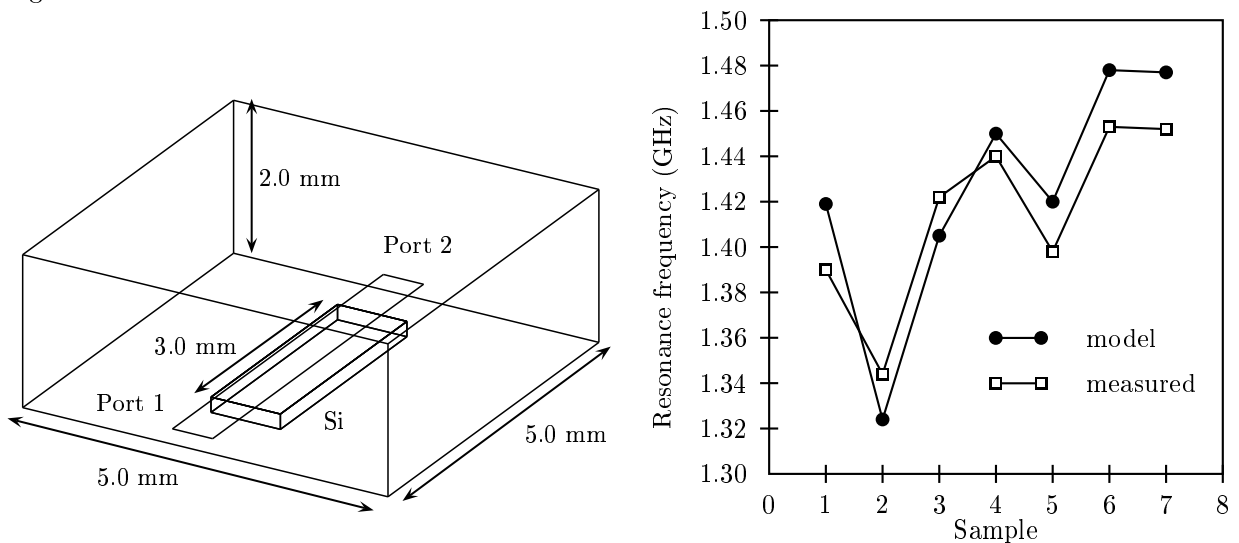


Figure 8: On the left the configuration in HFSS to verify the model for the capacitor. Shown on the right a comparison of measured and modelled resonance frequency.